Phosphorus deactivation mechanisms by hydrogenation in the n^+ emitter region and its effect on defects passivation in n^+pp^+ poly-silicon solar cells

R. Ouldamer[a,c], D. Belfennache[b,*], D. Madi[c], R. Yekhlef[b,d], S. Zaiou[e,f], Mohamed A. Ali[g].

[a]*Laboratory of Processes for Materials, Energy, Water and Environment, Mohand Oulhadj University Bouira, Algeria*

[b]*Research Center in Industrial Technologies CRTI, P.O. Box 64, Cheraga, 16014 Algiers, Algeria*

[c]*Physics of Materials and Optoelectronic Components Laboratory, Faculty of Sciences and Applied Sciences, Bouira University, P.O Box 10000 Bouira, Algeria*

[d]*Laboratory of Electrochemistry, Molecular Engineering and Redox Catalysis (LEIMCR) Department of Engineering Process, Faculty of Technology, Ferhat Abbas University Setif-1, Setif 19000, Algeria*

[e]*Emergent Materials Research Unit, Setif-1 University, 19000 Setif, Algeria*

[f]*Faculty of Natural Sciences and Life, Setif-1 University, 19000 Setif, Algeria*

[g]*School of Biotechnology,Badr University in Cairo(BUC), Badr City 11829, Cairo, Egypt*

Doping level of the n^+ emitter region is an essential parameter that controls the performance of the n^+pp^+ poly-silicon solar cells. Also, most poly-silicon n^+pp^+ solar cell manufacturers apply hydrogenation from the phosphorus emitter n^+ side to improve photovoltaic efficiency. Although hydrogen can passivate defects as well as it changes initial phosphorus doping level through phosphorus-hydrogen complex formation. Consequently, phosphorus deactivation can have a harmful effect on photovoltaic efficiency. In this context, the primary purpose of this work is to investigate the phosphorus deactivation in n^+ emitter region and its effect on defects passivation of hydrogenated n^+pp^+ poly-silicon solar cells. To do this, hydrogenation is performed by microwave plasma discharge involving an electron cyclotron resonance system. Besides, hydrogen passivates defects in poly-silicon, at the same time it deactivates phosphorus. For this reason, we have chosen to separate these simultaneous effects. So, we performed phosphorus deactivation on Schottky diodes-based mono-silicon, while defect passivation was operated in n^+pp^+ poly-silicon solar cells. Our results reveal that hydrogen effectively deactivates phosphorus dopant. This effect is deeper in Schottky diodes with low initial phosphorus doping level where hydrogen diffuses easily in the bulk. This behavior is clearly revealed in open circuit-voltage values (V_{oc}) measured on n^+pp^+ samples. In fact, solar cells with low phosphorus concentration in n^+ region revealed 319 mV compared to 230 mV for high doping level. Also, all n^+pp^+ poly-silicon solar cells show a saturation of V_{oc} at high microwave plasma power. Reasons for such case were explained and discussed in detail.

(Received October 25, 2023; Accepted January 8, 2024)

Keywords: Defect passivation, Poly-silicon, Hydrogen diffusion, Platelets, Silicon, Solar cells

1. Introduction

According to recent research, poly-silicon plays a significant role in a photovoltaic solar cell [1,2]. For such a material whose performance is limited by defects and impurities, it is

* Corresponding author: belfennachedjamel@gmail.com
https://doi.org/10.15251/JOR.2024.201.45

essential to be passivated using hydrogen to get higher energy conversion efficiency [3]. The gettering process will occur during the phosphorus diffusion required for n^+p junction creation [4]. It is a commonly used way of purifying the bulk of silicon wafers. Therefore, most silicon solar cell producers use hydrogenation from the n^+ emitter side to further eliminate the remaining electrically active defects. Hydrogen, on the other hand, reacts with phosphorus dopants to produce complexes [5, 6]. Consequently, the diffusion of hydrogen will be affected and will be the same for the passivation of the defects. Thus, efficient passivation of defects is only conceivable if phosphorus deactivation is understood and appropriately accounted [7,8].

Passivation of defects is usually achieved through the introduction of atomic hydrogen into silicon. This effect is of considerable complexity and remains a subject requiring much research to date [9]. However, the simplest picture to present is that hydrogen atoms mainly saturate the dangling bonds of point or extended defects thus generating an elimination of energy states in the bandgap space. Relatively, it there have been various studies carried out on the hydrogenation of silicon [10,11]. For this material, the most efficient hydrogenation process boils down to brief thermal annealing of a layer of hydrogen-rich silicon nitride (SiN:H) having been deposited by PECVD on the crystalline silicon surface [12,13].The advantage of this process on others is the double function of SiN: H namely as an anti-reflective layer and passing on the surface of the emitters of the solar cells and it is more practical because it also adapts well to the formation stages of photovoltaic cells [14].

In n^+pp^+ polysilicon photovoltaic structures, exposing the region of the n^+ emitter to the flow of hydrogen is a well-accepted technique for the passivation of defects and various impurities existing within the material. However, the amount of hydrogen introduced into the p region is greatly reduced by the presence of the n^+ layer doped with phosphorus [15-17]. Additionally, the photovoltaic efficiency of an n^+pp^+ cell made of polycrystalline silicon is much lower than that of monosilicon due to high defect concentrations, especially at the grain boundaries of the polycrystalline material. Consequently, to strengthen the potential offered by the polycrystalline silicon sector in photovoltaics, it is essential to carry out studies in order to understand the mechanism of neutralization of phosphorus in the region of the n^+ emitter for effective passivation of inter- and intra-grain.

In this work, the principal motivation is to examine the effect of phosphorus deactivation in n^+ emitter region on defects passivation of hydrogenated n^+pp^+ poly-silicon solar cells. Hydrogenation treatments are performed in an MW-ECR reactor where the plasma is generated by microwave discharge underneath an electron cyclotron resonance. The dopant activation/deactivation in Schottky diodes was measured via the C-V apparatus by studying the apparent doping phosphorus profile variation before and after hydrogenation.

2. Phosphorus deactivation and hydrogen diffusion in n-type silicon

Deactivation of donor atoms in silicon was first demonstrated by Johnson et al [18]. According to the literature [19] H^+ is a dominant species in hydrogen plasma. Moreover, hydrogen in n-type silicon comes in two atomic forms: H^- and H^0 [20]. Firstly, H^+ would be ionized by capturing an electron via:

$$H^+ + e^- \rightarrow H^0 \quad (1)$$

Therefore, H^0 absorbs a second electron from the surface to become H^- or capture another H^0 to form its molecule H_2:

$$H^0 + e^- \rightarrow H^- \quad (2)$$

The H^- ion is then attracted to the ionized P^+ donor atom to form a neutral complex with the following equation:

$$H^- + P^+ \xrightarrow{K_{PH}} PH \quad (3)$$

where K_{PH} is the coefficient of mobile hydrogen combination

$$K_{PH} = 4\pi r_C D_{H^-} \quad (4)$$

Equation 4 expresses the relative concentration of H^- and H^0 and is related to the location of the local Fermi level [20]:

$$\frac{[H^-]}{[H^0]} = \exp[(E_F - E_a)/K_B T] \quad (5)$$

where E_a is the acceptor energy level, E_F is the Fermi energy level, K_B is the Boltzmann constant, and T is temperature.

The thermal dissociation of PH complexes is strongly described by the reaction:

$$PH \xrightarrow{K'_{PH}} P^+ + H^-$$

while K'_{PH} is the dissociation coefficient [20].

After this partial dissociation of PH complexes, H^- absorbs a hole to become H^0, as follows:

$$H^- + h^+ \rightarrow H^0 \quad (7)$$

In addition, it is well admitted that the starting phosphorus doping level [$P_{starting}$] is equal to the active phosphorus concentration [P^+] at room temperature [21]. Consequently, after the hydrogenation process, the phosphorus deactivation concentration [PH] can be stated as:

$$[PH] = [P_{starting}] - [P^+] \quad (8)$$

The diffusion of hydrogen in n-type silicon follows Fick's law, where in one dimension the flux J(x) is proportional to the concentration gradient [H^0]:

$$J_{H^0}(x) = -D_{H^-} \frac{\partial [H^0]}{\partial x} \quad (9)$$

$$J_{H^-}(x) = -D_{H^-} \frac{\partial [H^-]}{\partial x} + D_{H^-}[H^-] \frac{1}{n} \cdot \frac{\partial n}{\partial x} \quad (10)$$

where D_{H^-} is the diffusion coefficient of hydrogen in n-type silicon.

For the determination of diffusion coefficients D_{H^-} by measuring the deactivation depth x_{H^-} and the duration of the hydrogenation process t_H. Based on a simple approximation:

$$x_{H^-} = \sqrt{D_{H^-} t_H} \quad (11)$$

The change in neutral complex PH concentrations is expressed by the following equation

$$\frac{\partial [H]^{Total}}{\partial t} = -\frac{\partial \left[J_{H^0} + J_{H^-}\right]}{\partial x} \quad (12)$$

$$\frac{\partial [PH]}{\partial t} = K_{PH}[P^+][H^-] - K'_{PH}[PH] \quad (13)$$

3. Capacitance – voltage measurements and extraction of doping profiles

Measurements of capacitance as a function of voltage C (V) are regularly used, because they make it possible to determine several parameters characteristic of metal/semiconductor

structures (Schottky diodes) or n^+p (pn junctions) and MOS (Metal Oxide Semiconductor). C (V) measurements are also very useful because they mainly make it possible to judge the quality of the structures studied. These measurements can be used to eliminate the contribution of interface states, when they are present in the determination of the doping profile [22]. In the following paragraphs, we will discuss briefly the derivations and equations required to extract doping profile by the C–V method.

$$C = \frac{dQ_S}{dV} \tag{14}$$

The neutrality equation of the semiconductor can be approximated by:

$$dQ_S = qAN_A(w)dw \tag{15}$$

The combination of equations (14) and (15) gives rise to

$$C = \frac{dQ_S}{dV} = qAN_A(w)\frac{dw}{dV} \tag{16}$$

We obtain equation (16) by neglecting the term dN_A/dV because N_A does not vary beyond the distance *dw*

On the other hand, the capacity of a plant junction is given by:

$$C = -\frac{K_S\varepsilon_0 A}{w} \tag{17}$$

where *w* is the width of the space charge region.

$K_S\ \varepsilon_0 = 11.7 \times 8.85 \times 10^{-12}\ Fm^{-1}$, A is the surface of the junction K_S and ε_0 are respectively the dielectric constant of the silicon and the vacuum permittivity [29].

$$N_A(w) = -\frac{C^3}{qK_S\varepsilon_0 A^2\left(\frac{dC}{dV}\right)} \tag{18}$$

$$N_A(w) = -\frac{2}{qK_S\varepsilon_0 A^2\left[\frac{d\left(1/C^2\right)}{dV}\right]} \tag{19}$$

The treatment of experimental data relating to the characteristic curve $C_{meas} = f(V_{appl})$ with equations (17), (18) or (19) are sufficient to determine the evolution of the deactivation profiles of active phosphorus depending on the depth x.

4. Experimental procedure

All Atomic hydrogen is required for effective passivation of defects in poly-Si. Indeed, it has been demonstrated that in order to passivate defects of in crystalline silicon (Si), atomic H is considered essential [23,24]. In other words, molecular hydrogen (H_2) is rather immobile in Si [25]. Therefore hydrogen must be introduced into the volume of Si in atomic form. For this purpose, several hydrogenation methods have been tested and optimized. In the following, the hydrogenation process is carried out in the MW-ECR plasma reactor of the ICUBE laboratory, University of Strasbourg, France. It is illustrated in the figure 1. A magnetic field is utilized to maintain the ECR condition, while 2.45GHz is used to ignite H_2 gas in the resonant chamber. At an H_2 of 30sccm and a hydrogenation time of 60 minutes, the plasma pressure was 0.6Pa. For a given substrate temperature of 200°C, the microwave plasma power (P_{MW}) was 650W.

For phosphorus deactivation we employed mono-crystalline silicon wafers (mc-Si) having 1cm×1cm in size, 280 µm thick, and uniformly doped with phosphorus at various starting levels. Prior to hydrogenation, all silicon wafers were cleaned using trichloroethylene (TCE), acetone, and methanol, treated in dilute hydrofluoric (HF) acid to eliminate native, followed by rinsing in

flowing deionized water and lastly drying in nitrogen flux. The mc-Si wafers were then hydrogenated in MW-ECR plasma reactor. Gold contacts of 1 mm diameter were deposited using a shadow metal mask onto the hydrogenated surface, while aluminum was deposited onto the rear face to provide an ohmic contact. Then, the Schottky diode was analyzed by capacitance-voltage apparatus at 1MHz and room temperature using a digital Hewlett Packard LCR meter controlled by a computer. The active phosphorus profile was calculated using these C–V data.

For defect passivation we used poly-silicon films, these films were prepared on thermal SiO_2 substrates by the Rapid Thermal Chemical Vapor Deposition (RTCVD) technique at atmospheric pressure and a temperature of 1080°C, using trichlorosilane and diborane as precursor and doping gas, respectively. Due to this process, two boron doped layers: p (base region) and p^+ (back surface field region) having thicknesses, respectively, of 3µm doped at 3×10^{16} cm^{-3} and 0.5µm doped at 5×10^{19} cm^{-3} are superimposed. The emitter n^+ region was formed by thermal diffusion of phosphorus at 900°C for 60 min from a doping source P507, P508 or P509. This will lead to a distribution of atoms based on the complementary error function (erfc) with a surface concentration ranging from $2x10^{20}$ to $2\times10^{21}cm^{-3}$ and a junction depth of about 0.5µm. Following the diffusion procedure, the samples are immersed in a HF hydrofluoric acid bath (5%) for two minutes to eliminate doping source oxide residues. Then, they are rinsed with deionized water and dried under nitrogen flux. A typical sheet resistance of 30-20 Ω/sq was measured by the four-point probe technique on the n^+ emitter region. Furthermore, the measurements of the open circuit voltage (V_{oc}) on our n^+pp^+ solar cells require the realization of the contacts with the emitter (n^+) and the back surface field (p^+). However, the presence of the SiO_2 insulating layer in the structure requires that all contacts be taken on the front side only, which leads to the formation of a mesa diode by the SCMP (side-contacted mesa process) process. Access to the p^+ region was achieved by reactive ion etching (RIE), where SF_6 gas etches the n^+p layer at a rate of 1,6 µm/min, forming a mesa cell.

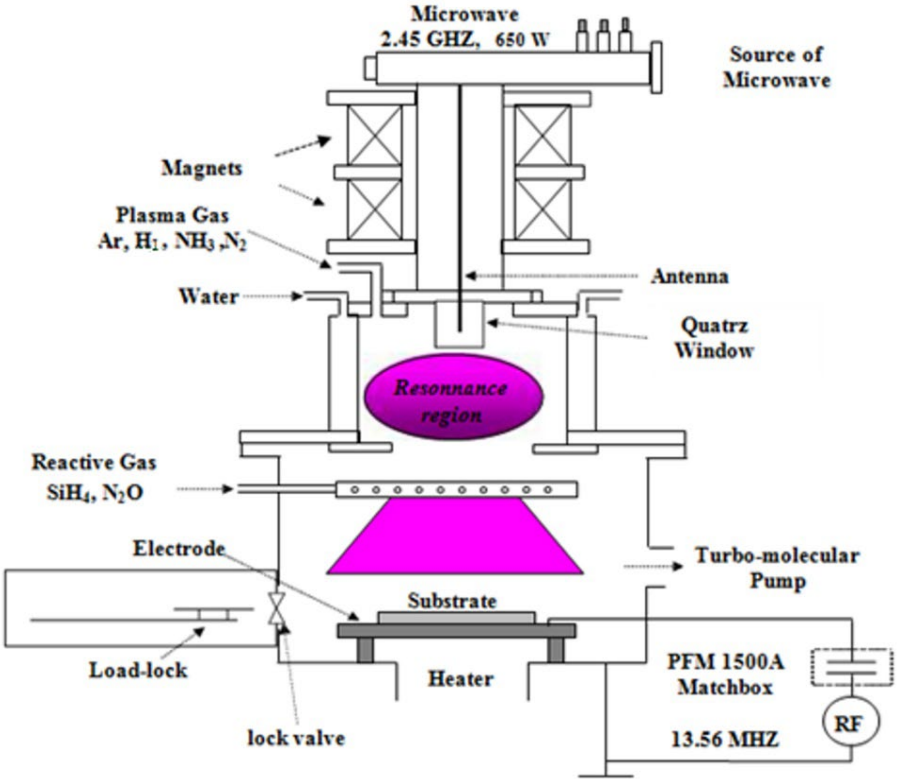

Fig. 1. Planning drawing of the reactor ECR-PECVD used in this work.

5. Results and discussion

5.1. Active Phosphorus Deactivation Profiles Evolution

The active concentration of phosphorus in monocrystalline silicon is a crucial parameter for defining the range of use of devices based on this material. Also, it has been shown that hydrogen (H) easily interacts with phosphorus which gives rise to a modification of their profiles due to the formation of hydrogen-phosphorus complexes [7]. In Fig.2, we will present the active phosphorus profile of mc-Si doped with different starting phosphorus level [$P_{starting}$] from 4×10^{13} to 2×10^{19} cm^{-3}. Also, the hydrogenation conditions are shown. We can observe the uniform phosphorus profile of the non-hydrogenated wafers. However, hydrogenation treatments affect the distribution and phosphorus level. In fact, our results show that increasing the starting phosphorus level of the samples leads to a reduction in the hydrogen-phosphorus diffusion fronts Xe, indicating the deep diffusion of hydrogen atoms in the bulk silicon with ($1/[P_{star.}]$). We notice that Xe = 0.75, 1.25, 3.68 and 9.93µm for [P_{star}] = 2×10^{19}, 7×10^{17}, 2×10^{15} and $4\times10^{13}cm^{-3}$, respectively. Also, the deactivation depth increased with the decreased of the starting phosphorus concentration. Consequently, our results show a hinder diffusion of hydrogen in the bulk of our samples.

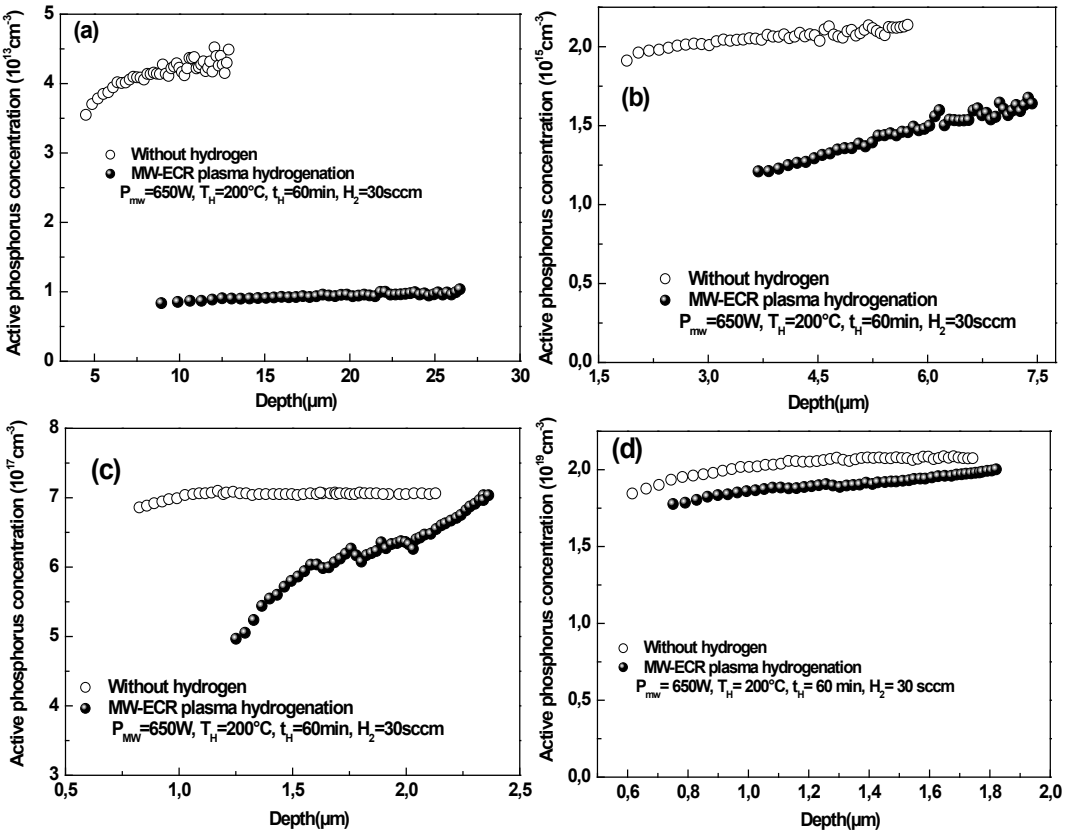

Fig. 2. Active phosphorus concentration profiles of hydrogenated of mc-Si wafers with different starting phosphorus level [$P_{star.}$] : (a) 4 x 10^{13}, (b) 2 x 10^{15},(c) 7 x 10^{17} and (d) 2 x $10^{19}cm^{-3}$.

Furthermore, our results show that for a specified quantity of hydrogenation, the concentration of neutralized phosphorus is directly proportional to the initial phosphorus concentration. So, the decimal logarithm of inactive phosphorus concentration (log[PH]) calculated at a depth of Xe in samples as a function of decimal logarithm of the starting phosphorus concentration (log[$P_{starting}$]) is shown in Fig.3. It assists to estimate the difficulty in diffusion of hydrogen in our n-type silicon. Hence, at higher concentrations of phosphorus, the [PH] tends to saturate.

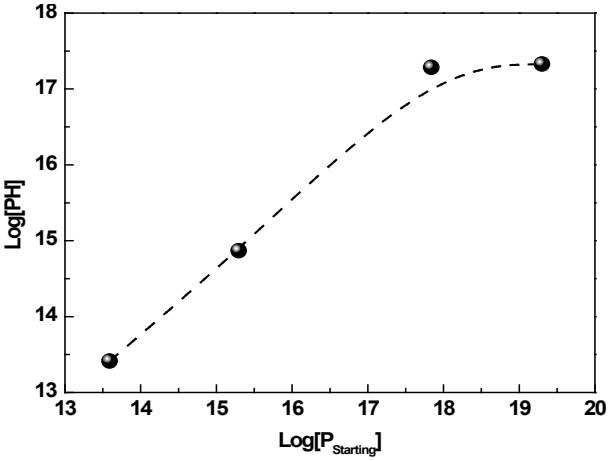

Fig. 3. Decimal logarithms of deactivated concentration of phosphorus at Xe depth versus the starting phosphorus concentration.

In order to demonstrate our statements, we calculated the diffusion coefficients in our samples corresponding to depth Xe through the relation (11). The results are shown in Fig.4. It reveals that phosphorus existence affects the diffusion coefficient (D_H^-) inversely, precisely for n-type silicon because of hydrogen–phosphorus complexes formation. These observations are in close agreement with those reported in the literature [20,26].

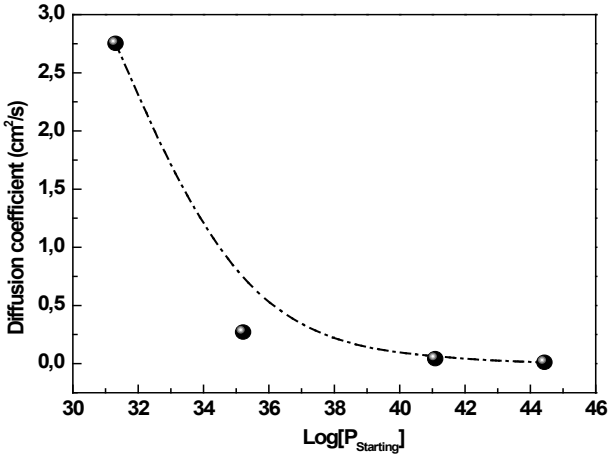

Fig. 4. Hydrogen diffusion coefficients calculated in mc-Si wafers doped with different phosphorus levels.

Analysis of all the research available in the literature shows that the interaction of hydrogen with silicon does not seem to be a simple phenomenon but rather more complex. In addition, the solubilities of the different species depend on the hydrogenation method used to amalgamate the hydrogen in silicon (molecular hydrogen atmosphere, hydrogen plasma, deposition of hydrogen-rich layers such as SiN:H , ion implantation, electrochemical solution, etc.) which is often difficult to characterize. Nevertheless, it is often reported that depending on the position of the Fermi level, atomic hydrogen in silicon can be in a positive, negative, or neutral charged state. Also, the presence of molecular hydrogen (H_2) has often been cited. As a result, at least three species appear to be present in n-type silicon (H_2, H^0 and H^-). Their stability is determined from the hydrogenation method chosen [27, 28] while the quantity relative to each species varies with the temperature and the doping level. Furthermore, we assume that at a given temperature, the diffusivity relative to each species in intrinsic silicon increases according to the order of the species classified below: H_2, H^0 and H^- in type n. Actually, it is well-known that the principal species in MW-ECR plasma system is H^+ which impinges the substrate surface as a

result of magnetic field and sheath potential [29]. Also, above ambient temperature the charge state of hydrogen (H^+, H^- and H^0) depends on the Fermi level position in the band gap of silicon and H^+ changes to H^- through the state configuration of H^0 [30,31]. In addition, it is possible that H^0 captures an electron or another H^0 to produce respectively hydrogen negative or its molecule. These molecules seem as platelets at the subsurface layer of silicon [32-34]. Because platelet nucleation occurs at phosphors sites, the platelets concentration improves monotonically as silicon's phosphorus content increases [35]. Furthermore, Huang et al. has reported that platelets size depends on the hydrogen diffusivity in the silicon although the platelets reduce the in-diffusion of hydrogen [26]. Thus, based on what that mentioned above, we can state that hydrogen H^+ absorb an electron at the sample surface to become H^0 ($H^+ + e^- \rightarrow H^0$) and the H^0 would be ionized by capturing a free electron ($H^0 + e^- \rightarrow H^-$) and then phosphorus deactivation would progress with $H^- + P^+ \rightarrow PH$. When phosphorus concentration increases, the densities of H^0 and H^- become significant. This resulted in high amounts in phosphorus deactivation and larger dimension of platelets. So, the platelets prevent hydrogen from diffusing deeply into the samples. However, decreasing the phosphorus concentration induces a low amount of H^- and probably a dispersion of H^0 on the sample surface. Therefore, the platelets amount will be little, which allows H^- diffusion as well as a deep phosphorus deactivation in silicon.

5.2. Defects Passivation Behavior

Grain boundary activity can be demonstrated by measuring the open-circuit voltage (V_{oc}) on n^+pp^+ polysilicon (poly-Si) solar cells. The results obtained are shown in Table 1. It is clearly seen that the V_{oc} values measured are much lower for P509 compared to P507. This observation is explained by the fact that during emitter formation on polycrystalline films, two phenomena are responsible for improving the electrical properties of the material. This is the passivation by phosphorus of grain boundary defects and removal of impurities by Getter effect from the poly-Si bulk to inactive areas of the device [36,37]. However, increasing the phosphorus doping level in emitters region give rise a high surface recombination velocity leading to the degradation of V_{oc}.

Table 1. Open-circuit voltage measured on polysilicon based solar cells for doping sources P507, P508 and P509. Thermal diffusion of phosphorus to form the emitter region n^+ was performed at 900°C during 60 min.

	Open-circuit voltage : V_{OC} (mV)		
Doping sources	P507	P508	P509
Poly-Si : n^+pp^+	170 ± 5	155 ± 5	125 ± 5

The influence of microwave plasma power P_{MW} on the cell device parameters was studied. Open-circuit voltage (V_{oc}) is measured as a function of microwave plasma power (P_{MW}). Results are shown in Fig.5.

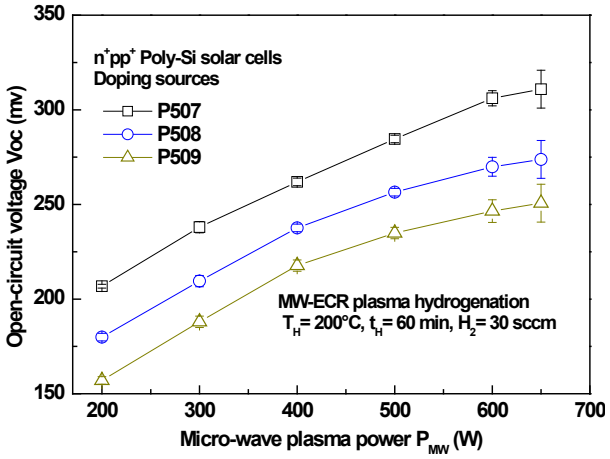

Fig. 5. Open-circuit voltage versus MW plasma power measured on pc-Si n^+pp^+ mesa cells.

A considerable and continuous increase of V_{oc} was observed for the three doping sources, P507, P508, and P509 of the n^+ emitter region, after 60 min of hydrogenation treatment at 200°C. As mentioned, the V_{oc} values are higher for P507 than for P508 or P509. This behavior is induced by the decrease of hydrogen diffusion due to the formation of PH complexes. Also, we can see the tendency of V_{oc} to saturate at high microwave plasma power for all cells. This situation is probably related to the accumulation of molecular hydrogen beneath the n^+ surface, which strongly hinders the hydrogen diffusion in the bulk [17,35]. As reported in other works [38,39], the improvement in open circuit voltage after hydrogenation is mainly due to the neutralization or passivation of defects at grain boundaries and inside the grains (dislocations) of polycrystalline silicon films. This is accomplished by the fact that high doses of atomic hydrogen diffuse across the surface of the n^+ emitter into the silicon volume from the plasma environment. The latter, according to [40], is the seat of considerable quantities of H^0, H^+ and H_2.

6. Conclusion

In this work, we investigate the effect of phosphorus deactivation in n^+ emitter region on defect passivation of hydrogenated n^+pp^+ poly-silicon solar cells. To do this, we suggest to examine separately these two effects. Thus, we carried out MW-ECR plasma hydrogenation treatments on n^+pp^+ poly-silicon solar cells and Schottcky diodes-based mono-silicon to follow respectively the open-circuit voltage (V_{oc}) behavior and the phosphorus deactivation profile evolution. Our results show that V_{oc} values increase significantly when the microwave plasma power (P_{MW}) is high. V_{oc} is considerable for low doped emitter region. This behavior is correlated to phosphorus deactivation by hydrogen. In fact, phosphorus impedes hydrogen diffusion in bulk of cells due to the formation of PH complex. As well, we observed V_{oc} saturation at high P_{MW}. This observation is as expedite as the initial phosphorus concentration in emitter is high. This finding is explained by the formation of molecular hydrogen plans closer to the silicon surface called platelets, which increase with increasing phosphorus concentration. In this case, H^+ becomes H^0 to promote interaction with another H^0 instead of gaining an electron to convert to a negative ion H^-, the primary diffusion species in n-type silicon. As well, this statement is further confirmed with the values of hydrogen diffusion coefficient D_{H^-} estimated at the hydrogen-phosphorus diffusion fronts. Finally, due to the vast complexity of hydrogen diffusion and phosphorus deactivation in the highly inhomogeneous material polycrystalline silicon, several issues are still open for future investigation in order to fully understand the abilities and limitations of defects passivation. Hopefully, the results presented in this work gives a contribution to this understanding.

References

[1] J. Yu, Y.Chen, J. He, Y. Bai, R. Su, T. Cao, W. Liu, T. Chen, Sol. Energy Mater Sol. Cells. 260. 112491 (2023); https://doi.org/10.1016/j.solmat.2023.112491
[2] P. K. Enaganti, P. K. Dwivedi, A. K. Srivastava, S. Goel, Solar Energy, 211. 744-752 (2020); https://doi.org/10.1016/j.solener.2020.10.025
[3] B. J Hallam, P.G. Hamer, A.M. Ciesla, C.E. Chan, B. V. Stefani, S. Wenham, Prog. Photovolt.: Res. Appl. 28 (12). 1217-1238 (2020); https://doi.org/10.1002/pip.3240
[4] B. Hallam, D. Chen, M. Kim, B. Stefani, B. Hoex, M. Abbott, & S. Wenham, Phys. Status Solidi A, 214(7). 1700305 (2017); https://doi.org/10.1002/pssa.201700305
[5] A. Endrös, Phys. Rev. Lett, Vol. 63(1). 70-73 (1989); https://doi.org/10.1103/PhysRevLett.63.70
[6] D. Belfennache, D. Madi, R. Yekhlef, L. Toukal, N. Maouche, M.S. Akhtar, S. Zahra. Semicond. Phys. Quantum. Electron. Optoelectron. 24(4). 378-389 (2021); https://doi.org/10.15407/spqeo24.04.378
[7] D. Belfennache, N. Brihi, D. Madi, Proceeding of the IEEE xplore, 8th (ICMIC) (2016) 7804164. 497–502 (2017)

[8] R. Ouldamer, D. Madi, D. Belfennache, In: Hatti, M. (eds) Advanced Computational Techniques for Renewable Energy Systems. IC-AIRES 2022. Lecture Notes in Networks and Systems, 591. 700-705 (2023) Springer, Cham. https://doi.org/10.1007/978-3-031-21216-1_71
[9] A. Soman, A. Antony, Appl. Surf. Sci. 553. 149551(2021) ; https://doi.org/10.1016/j.apsusc.2021.149551
[10] T. O. Abdul Fattah , V. P. Markevich , D. Gomes, J. Coutinho, N. V. Abrosimov, I. D. Hawkins, M. P. Halsall, A. R. Peaker, Sol. Energy Mater Sol. Cells. 260. 112447 (2023); https://doi.org/10.1016/j.solmat.2023.112447
[11] A. Abdurrazaq, A. T. Raji , W. E. Meyer, Mater. Sci. Semicond. Process. 110. 104967(2020); https://doi.org/10.1016/j.mssp.2020.104967
[12] A. Focsa, A. Slaoui, H. Charifi, J.P. Stoquert, S. Roques, Mater. Sci. Eng. B. 159–160, 242-247 (2009); https://doi.org/10.1016/j.mseb.2009.02.009
[13] A. El Amrani, A. Bekhtari, A. El Kechai, H. Menari, L. Mahiou, M. Maoudj, Vacuum. 120. 95–99 (2015); https://doi.org/10.1016/j.vacuum.2015.04.041
[14] D. Madi, A. Focsa, S. Roques, S. Schmitt, A. Slaoui, B. Birouk. Energy Procedia. 2. 151–157(2010). https://doi.org/10.1016/j.egypro.2010.07.021
[15] D. Madi, B. Birouk Int. J. Sci. Res. Publ. 4(4). 1-6(2014)
[16] D. Madi, P. Prathap, A. Slaoui. Appl. Phys. A. 118. 231–237(2015); https://doi.org/10.1007/s00339-014-8665-z
[17] S. Mahdid, D. Belfennache, D. Madi, M. Samah, R. Yekhlef, Y. Benkrima. J. Ovonic. Res. 19(5). 535-545 (2023); https://doi.org/10.15251/JOR.2023.195.535
[18] N.M. Johomson, M.D. Moyer, Appl. Phys. Lett. 46. 787–789(1985); https://doi.org/10.1063/1.95883
[19] E. Hyman, K. Tsang, A. Drobot, B. Lane, J. Casey, R. Post, J. Vac. Sci. Technol. A. 12. 1474 (1994); https://doi.org/10.1116/1.579340
[20] R. Rizk, P. Mierry, D. Ballutand, M. Aucouturier, D. Mathiot, Phys. Rev. B. 44. 6141–6151 (1991); https://doi.org/10.1103/PhysRevB.44.6141
[21] D.K. Schroder, Semiconductor Material and Device Characterization, New York: John Wiley & Sons Inc. Hoboken, 2006.
[22] R. Ouldamer, D. Madi, D. Belfennache, In: Hatti, M. (eds) Advanced Computational Techniques for Renewable Energy Systems. IC-AIRES 2022. Lecture Notes in Networks and Systems, 591. 700-705 (2023) Springer, Cham; https://doi.org/10.1007/978-3-031-21216-1_71
[23] D. Belfennache, D. Madi, N. Brihi, M. S. Aida, M. A. Saeed, Appl. Phys. A. 124. 697 (2018); https://doi.org/10.1007/s00339-018-2118-z
[24] T. N. Truong, D. Yan, C. Samundsett, A. Liu, S. P. Harvey, M. Young, Z. Ding, M. Tebyetekerwa, L.Li, F. Kremer, M. Al-Jassim, A. Cuevas, D. Macdonald, H. T. Nguyen.. ACS Appl Energy Mater . 2. 8783 (2019); https://doi.org/10.1021/acsaem.9b01771
[25] A.W.R. Leitch, V. Alex, J. Weber. Solid State Commun. 105(4). 215-219(1998) https://doi.org/10.1016/S0038-1098(97)10107-7
[26] Y.L. Huang, Y. Ma, R. Job, W.R. Fahrner, Appl. Phys. Lett. 86. 131911–1319113 (2005). https://doi.org/10.1063/1.1896443
[27] A.W. R. Leitch, V. Alex, J. Weber, Phys. Rev. Lett. 81, 421 (1998). https://doi.org/10.1103/PhysRevLett.81.421
[28] K. Murakami, N. Fukata, S. Sasaki, K. Ishioka, M. Kitajima, S. Fujimura, J. Kikuchi, H. Haneda, Phys. Rev. Lett 77, 3161 (1996); https://doi.org/10.1103/PhysRevLett.77.3161
[29] S.F. Yoon, K.H. Tan, Q. Zhang, M. Rusli, J. Ahn, L. Valeri, Vacuum, 61, 29-35 (2001). https://doi.org/10.1016/S0042-207X(00)00429-2
[30] P. Hamer, B. Hallam, R.S. Bonilla, P.P. Altermatt, P. Wilsham, S. Wenham, J. Appl. Phys, 123, 043108 (2018); https://doi.org/10.1063/1.5016854
[31] C. Herring, N.M. Johnson, C.G. Van de Walle, Phys. Rev. B, 12. 125209 (2001).
[32] C.G. Van de Walle, Y. Bar-Yam, S.T. Pentelides, Phys. Rev. Lett. 60. 2761–2764 (1988); https://doi.org/10.1103/PhysRevLett.60.2761
[33] P. Deák, L.C. Snyder, J.L. Lindström, J.W. Corbett, S.J. Pearton, A.J. Tavendale, Phys.Lett. A. 126. 427–430 (1988); https://doi.org/10.1016/0375-9601(88)90805-

[34] Y. Ma, Y.L. Huang, W. Dünger, R. Job, W.R Fahrner, Phys. Rev. B, 72. 085321 (2005); https://doi.org/10.1103/PhysRevB.72.085321
[35] N.H. Nickel, G.B. Anderson, N.M. Johnson, G. Walker, Phys. Rev.B, 62. 8012–8015 (2000); https://doi.org/10.1103/PhysRevB.62.8012
[36] H.T. Nguyen, S. Mokkapati, D. Macdonald, IEEE Journal of Photovoltaics, 7(2). 598-603(2017); https://doi.org/10.1109/JPHOTOV.2017.2650561
[37] K. Adamczyk, R. Sondena, G. Stokkan, E. Looney, M. Jensen, B. Lai, M. Rinio, M.D. Sabatino, J. Appl.Phys. 123. 055705 (2018); https://doi.org/10.1063/1.5018797
[37] A. Slaoui, E. Pihan, I. Ka, N. A. Mbow, S. Roques, J. M. Koebel, Sol. Energy Mater. Sol. Cells. 90. 2087-2098 (2006); https://doi.org/10.1016/j.solmat.2006.02.004
[38] D. Madi, P. Prathap, A. Focsa, A. Slaoui, B. Birouk, Appl. Phys. A. 99, 729–734 (2010) https://doi.org/10.1007/s00339-010-5623-2
[39] E.S. Cielaszyk, K.H.R. Kirmse, R.A. Stewart, A.E. Wendt, Appl. Phys. Lett. 67, 3099-3101 (1995); https://doi.org/10.1063/1.114877